New Mauna Loa coronagraph systems

R. R. Fisher, R. H. Lee, R. M. MacQueen, and A. I. Poland

A new set of instruments, consisting of two coronagraph systems, has been installed and is operating at the Mauna Loa Observing Station, Hawaii, operated by the High Altitude Observatory of Boulder, Colorado. The instruments are the 23-cm objective Mark III K-coronameter (K-III) system, a photoelectric instrument used to observe the inner solar corona from 1.2 R_0 to 2.2 R_0 and the 12.5-cm objective Prominence Monitor system used for the detection of H_α limb activity. New features of the K-coronameter system include the use of achromatic wave plates for wide bandpass operation and linear diode array detectors. Raster scans of the coronal image are obtained in 1.5 min for a critical sampling scheme of 20-sec of arc resolution (10 × 10-sec of arc pixels) in the coronal pB image. This represents a 350 information gain factor for each detection channel when compared with the previous Mauna Loa K-coronameters.

I. Purpose of the Mauna Loa System

Until the fall of 1978, the inner white light corona was observed at times other than total solar eclipse using K-coronameters, two of which were located on Mauna Loa, Hawaii.[1,2] These two instruments were single-point scanning devices which required ~2 h of observing time to construct a single image of the corona with a spatial resolution of 2–4 min of arc. To improve both the temporal and spatial resolutions so that transient coronal activity might be observed between 1.2 R_0 and 2.2 R_0, the design, construction, and installation of a third (hence the name Mark III) K-coronameter was undertaken by the High Altitude Observatory (HAO) in the fall of 1974.

The principal goal of the Mauna Loa experiment is the collection of data concerning coronal and prominence activity during the maximum phase of solar cycle 21, 1980–1981. To be significant, these data must have sufficient temporal and spatial resolutions, coupled with photometric accuracy, so that changes in the mass and energy content of the corona may be correctly estimated. These changes may occur in relatively brief periods of time, such as minutes to hours in the case of transient activity, or over periods of days to months, as evolutionary changes in the coronal form. A distinction between two different kinds of observing task must be made. First, there are those tasks which require quantitative data, e.g., the scientific data tasks. These include collection of appropriate data such that (a) changes in mass and energy content of the solar atmosphere that are associated with increase of solar transient activity around sunspot maximum may be defined, and (b) definition of the long term changes in the density structure of the solar corona may be carried out.

A second observing task centers around the observational goals of the HAO coronagraph/polarimeter onboard the NASA solar maximum mission (SMM). Like its externally occulted predecessors on 0S0-7, ATM Skylab and P78-1 missions, the coronagraph/polarimeter is unable to observe the inner coronal regions. This is a consequence of the externally occulted coronagraph configuration. To take advantage of the low sky background afforded by the space environment, an externally occulted coronagraph design is optimal for fields of view beginning at approximately 1.5 $R_\odot$ (from sun center) and extending outward. Thus the onset and early development of many events in the coronar are not visible to the spaceborne instruments, and a second kind of observational task can be identified, that of collection of coronal and prominence data on a real-time basis so that proper pointing of the SMM instrument may be accomplished.

II. Experiment Systems

The system, which meets the requirements set by the scientific and observational tasks, consists of two telescopes mounted on a single 3.04-m long spar: a K-coronameter with a 23-cm diam objective lens and an H_α telescope with an objective diameter of 12.5 cm. These are located at the HAO Mauna Loa site, island of Hawaii, at an altitude of 3440 m. The 3-m spar is pointed at the center of the sun by a two-axis servo system, the spar guider. The signal for this system is developed in an independent telescope attached to the side of the main K-III instrument. There is mounted

The authors are with National Center for Atmospheric Research, High Altitude Observatory, Boulder, Colorado 80307.

Received 6 November 1980.
0003-6935/81/061094-08$00.50/0.

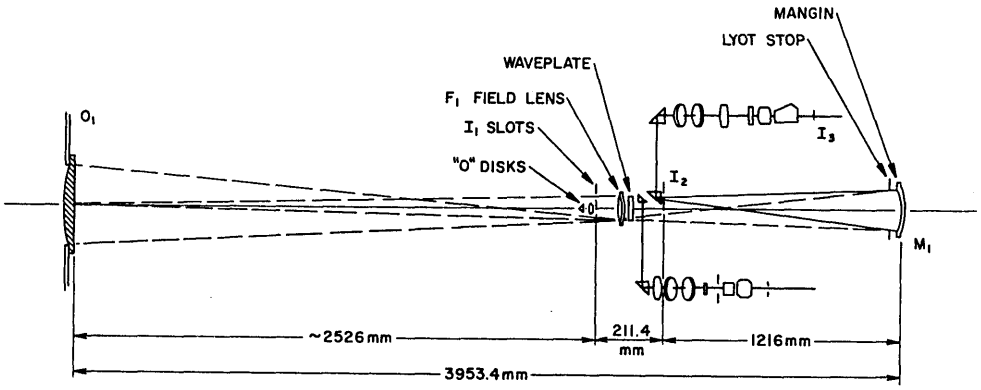

Fig. 1. Mark III optical schematic.

on the spar another small telescope which is used to measure the product of the solar brightness at the center of the sun's disk and the transmission of the earth's atmosphere.

The K-coronameter uses an optical system designed for low scattered light and relatively wide spectral bandpass. The polarized component of the scattered light of the sky, the polarized components of the electron corona and the F-corona are modulated by means of a rotating achromatic halfwave plate and calcite beam splitting prisms. The corona is observed in the passband from 7000 to 10800 A by moving the detector systems in the final focal plane. The image is scanned by placing the linear detector arrays normal to the limb and then rotating the entire detection system in solar position angle about the center of the solar disk. The time required to obtain one complete, critically sampled scan with 20-sec of arc resolution is 1.5 min. Data are recorded on nine-track magnetic tape, 1600 bits/in., phase encoded.

The 12.5-cm limb monitoring system has a field of view 2.0 R_0 from sun center when the instrument is pointed at sun center; offset pointing can increase the field of view to ~3.5 R_0 at one selected limb. The telescope feeds a video camera system and a 35-mm Acme film camera. Limb observations are made using a series of 8-A FWHM bandpass interference filters centered at or near H_α with an occulting system interposed at the initial image plane. Disk observations are made using a 0.5-A H_α filter without occulting. Images are recorded on photographic film for subsequent microdensitometer reduction at the data base in Boulder, Colo. These provide velocity information on active limb events both in the plane of the sky and (with certain assumptions) in the line of sight.

III. 23-cm K-Coronameter (K-III)

The K-III telescope is a conventional singlet-objective coronagraph which uses a second surface mirror (Mangin mirror) to relay the primary chromatic image to an achromatic focus at the second image plane. A similar design was described by Rush and Schnable.[4] The optical path is shown in Fig. 1.

The objective lenses are fabricated from Schott BK-7 material, selected so as to be as free from bubbles and striae as possible. The objectives are plano-convex with the flat side toward the occulting disk. The objective forms a chromatic image near I_1. The back focal length of the O_1 λ6328 A is a nominal 2500 mm from the last surface of the lens, the λ11000-A focus is almost 50.5 mm longer.

The secondary system consists of a field lens and the Mangin mirror. The field lens is a doublet which is used to transfer an image of the objective aperture onto the Lyot stop, A_2, placed just in front of the Mangin mirror. A second task for the field lens—that of color correction—requires that the principal plane of the objective be imaged rather accurately onto the principal plane of the Mangin mirror. The Mangin mirror relays the image from I_1 to I_2. Since it has a dispersive power which is just equal but opposite in sign to the objective lens, the I_2 image is accurately achromatized, with the same longitudinal focus at all wavelengths and very little lateral color between 6500 and 9600 A. The system is relatively free from geometrical aberrations. Spherical aberration of the O_1 lens is nearly corrected by the mirror M_1, the system is almost coma free, and the major off-axis aberration is astigmatism. Total system aberration results in theoretical and measured spot size considerably <1 K-III pixel element at 1.5 R_0.

Tertiary systems are used to relay I_1 to the focal planes and detector arrays. The incoming polarized light is frequency and phase encoded by a rotating, achromatic modulator plate placed behind the I_1 occulting disk assembly. A single Polaroid placed behind a rotating wave plate results in the Stokes parameters Q (polarization parallel and perpendicular to the polarizer axis) and U (polarization at ±45° to the reference axis) being sine (U) and cosine (Q) modulated at four times the angular velocity of the halfwave plate. If I_{obj} is the brightness of a given source at an object point, the modulated fluctuation of intensity in the image plane is

$$I_{image}(t) = 0.5[I_{obj} + Q\cos(4\omega t) + U\sin(4\omega t)],$$

where Q and U are the Stokes parameters characteristic of linear polarization,[5] and ω is the angular velocity of the wave plate. If the measurement axis is chosen tangent to the limb of the sun, it is possible to redefine

Q and U to be non-normalized quantities which are proportional to the polarized brightness signals of interest.

$$Q = pB_K + pB_F + pB_1 = I(0°) - I(90°),$$

$$U = pB_2 = I(45°) - I(135°),$$

where pB_K is the K-corona component,
pB_F is the F-corona contribution,
pB_1 is the result of primary sky scattering, and
pB_2 is the secondary sky scattering component.
A review of sky polarization detected with the K-coronameter is given by Leroy *et al.*[6]

The second image is formed at I_2 and is relayed to the final image plane by a series of prisms working at total internal reflection. The beam encounters two 90° internal reflection prisms, the two-plate polarization compensator system, a second field lens, the third objective, and finally a beam splitting prism. The beam splitting prisms in this case are Foster modifications to the Glan-Thompson prism, and these are made from calcite. The final focus is at I_3, where the initial defining slit at I_2 is brought to focus on the two sets of Reticon detectors.

The defining slits are not located at I_1 in order to avoid introducing a partial polarization of the incoming beam with a single narrow slit.[7] The beam is actually only occulted at I_1 at a wavelength of ~8200 A, and the coronal light passes through slots in a mask located just behind the occulting disk. Thus, the initial beam is converted to separate smaller beams each placed radially and located at intervals in azimuth about the occulting disk of 30°. After passing through the modulator and secondary system, an image of the five defining slots is formed into five defining slits at I_2. These slits are actually triangular in shape having a width of ~20 sec of arc at a distance of 2.33 R_0 from the center of the sun, while the width at 1.04 R_0 is 3 sec of arc. The image scale has been adjusted so that each diode of the Reticon arrays subtends 10 sec of arc in the radial direction, and the azimuthal extent is defined by the slit at I_2. Each channel has an independent set of tertiary optics and a Reticon detector pair. The optical bandwidth of this system is defined by a short wavelength cutoff filter (Schott RG-695) and the long wavelength cutoff of the Reticon detectors. This means that the effective wavelength of the system is ~8200 A, and the total width of the detection system ranges from ~7000 to ~10800 A. At the present stage of the instrument development, four of these channels are dedicated to this broad bandpass.

The objective lens is both rotated and translated. The lens is rotated at the same rate as the slit assembly at I_2 scan rate about the solar limb. This is done to minimize the effects of changes in instrumental polarization as a function of scan position in the coronal image. The lens is also translated so as to compensate for the elastic behavior of the spar as well as large, fast image motions due to seeing variations. A pair of spherical occulting disks with different radii of curvature are used to deflect part of the initial disk beam into the O_1 guider sensors, which are located in front of the modulator and I_1 area. This O_1 servo system is rather fast, operating from dc to 25 Hz.

A two-plate calibrator is located in front of the occulting disk between the objective lens and the initial image plane. The calibrator (not shown in the optical diagram) consists of a two-plate partial polarizer with adjustment in both tilt of the plates (degree of polarization) and azimuth of the partial polarizer. A diffuser is located in front of the O_1, and the combination of the diffuser and the tilt plate assembly gives a sufficient range in pB so that instrument calibration, gain, and dark current tables may be calculated for each diode pair. A shutter and neutral density filter are also included in the calibrator fixture.

IV. Linear Diode Arrays

Each K-III channel consists of two Reticon linear diode arrays positioned at the tertiary image. Each array contains 128 diodes. The beam splitting prisms are used to form identical images on each pair, with the exception that one Reticon is exposed to light polarized parallel to a unique axis, and the other is exposed to light polarized perpendicular to this axis. In the case of K-III this axis is normal to the limb of the sun for each of the six array channels. Light is allowed to fall on the array pair for a fraction of the modulator rotation period. A charge is built up on each diode which is proportional to the amount of flux per integration period and the quantum efficiency $n(\lambda)$. The arrays are read out so that the charge pairs are used to find the sun and difference between the nth diode pair. The values are then made available to a digital demodulation system. A systems diagram is shown for the K-III in Fig. 2. A discussion of image sensing with similar arrays is given by Livingston *et al.*[8] A single sample consists of an analog integration over $1/64$ of one full rotation of the modulator; the modulator rotates once every $4/30$th of a second or 133 msec. The diode pairs are allowed to integrate for ~2 msec. The difference between diode pairs is proportional to the K-coronal pB signal in the case in which the modulator axis is located parallel and perpendicular to the limb and is proportional to the pB signal of the sky (secondary scattering of air molecules after an initial reflection off the surface of the earth, ocean, etc.). The sum of the two samples is proportional to the average total flux falling on the diode pairs.

The signal-to-noise ratio of the detectors is limited in the high flux limit by the statistics of the incident photon field and by the noise equivalent charge associated with the diode read process. In the K-III instrument, the inner portion of the image is bright enough to approach the first limit, and a second consideration of the total charge capacity per diode becomes a consideration. The diode is capable of storage of $\sim 2 \times 10^7$ hole–electron pairs, so that the flux must be limited to flux of $\sim 2 \times 10^7$ photons per integration period per pixel, or saturation of the array pairs will occur. A summary of signal noise for expected telescope performance, a model corona, and the measured charac-

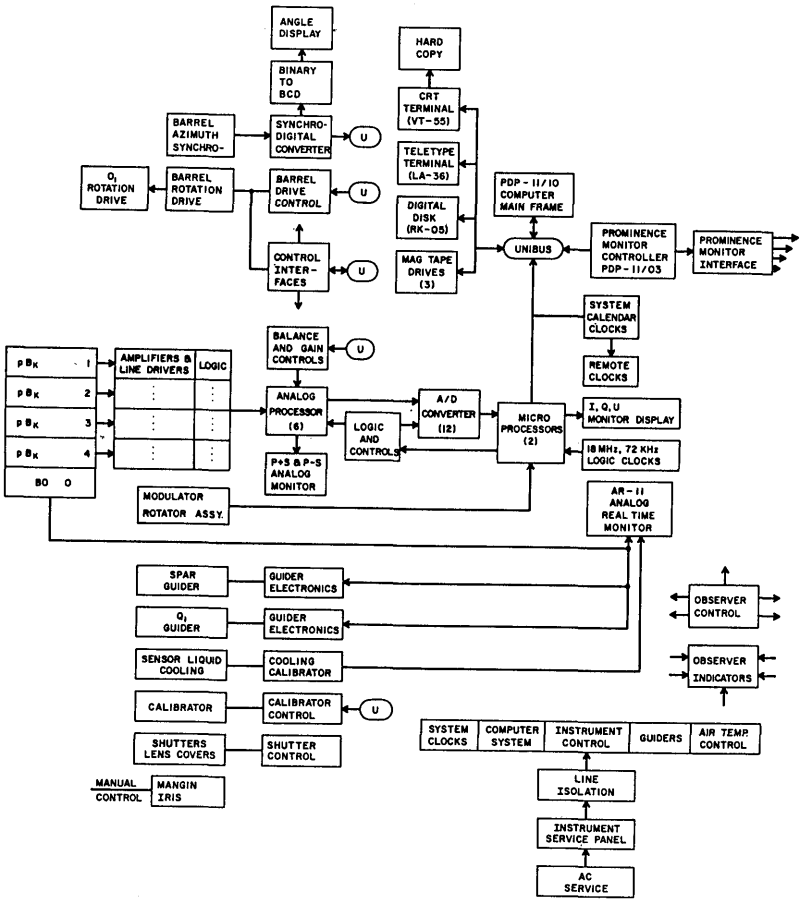

Fig. 2. Mark III electronic systems diagram.

Table I. Mark III Expected and Measured Signal-to-Noise Values

P Height above the limb (R_0)	Model I_{K+F} brightness (B_0 erg sec^{-1} cm^{-2} sr^{-1})	Model p_{equator} polarization	Model of pB_{equator} expected ($-10^{-8}\,B_0$)	Expected flux (photoelectrons sec^{-1} pixel)[a]	SNR_{rms} (expected for 10^{-5} B_0 sky)	SNR_{rms} (measured)
1.20	5.64 E-07	0.35	1.97 E + 01	3.64 E + 06	39	28
1.40	1.67 E-07	0.37	6.2	1.14 E + 06	12	14
1.60	7.10 E-08	0.40	2.3	1.02 E + 06	11	12
1.80	3.54 E-08	0.35	1.2	1.14 E + 06	12	8
2.00	2.08 E-08	0.30	6.2 E − 01	7.34 E + 05	8	2

[a] Includes effects of triangular sample slit.

teristics of the Reticons is given in Table I. The observed SNR is lower than the expected estimate because of image motion caused by seeing variations and modulator rotation. A liquid cooling system was built into each detector pair to eliminate detector variations as a function of temperature. This system was not intended to reduce the dark activity of the detectors, but was rather simply intended as a means of minimizing daily variations in the performance of the diodes. By inspection of the data, it seems that the thermal changes do cause a small variation in sensitivity, of the order of 3% in amplitude, as a function of time, but this changes slowly during any given day. Thus the cooling system is neither required nor is it presently used.

V. Analog System

After an initial reading of the charge pairs for each K-III channel, the analog system is used to convert the sum and difference amplifier outputs to digital values for transmission to the digital demodulation system. This system is a double correlated sampling system which is phase locked to the azimuthal position of the rotating halfwave plate. Each channel's analog system is also responsible for three other functions. The system bandwidth is limited on the high frequency end as well as rejecting low frequency ($1/f$) noise. And finally, differences in diode pair sensitivity are corrected by applying a (digital) gain and dark current correction table to the analog system through a set of multiplying

digital-to-analog converters. The gain and dark current tables are developed during the calibration process using the PDP-11/10 control computer, and these are then entered into the analog system. Data words are presented to the digital system as 12-bit words.

VI. Digital System

The digital system consists of a clock, two bipolar bit-slice microprocessor demodulation computers, and peripheral devices which are able to communicate from the microcomputers to the analog subsystem and PDP-11/10 memory. At the end of the ADC process by the analog system, data words are presented to the digital system. These are double buffered into microprocessor memory and then manipulated so that the frequency and phase encoded information concerning Q and U are correctly demodulated.

A period of 0.133 sec is required for one complete rotation of the wave plate. During this time there are four complete linear polarization modulation cycles for the polarized component of the K-corona. Each modulation cycle is divided into sixteen separate sample periods, each ~0.002 sec long. The diode pairs are read, digitized, and a digital demodulation algorithm applied by the microprocessor system. A summation over four complete cycles is then performed so that variations in the wave plate may be averaged to zero. The microprocessors finally write three data words (16 bits long) for each full rotation of the wave plate, summation over 64 discrete diode array samples. It must be remembered that Q and U are non-normalized Stokes parameters, and they are generally proportional to the K-coronal signal and the secondary sky signal, respectively. Since both the barrel rotation and the integration within the Reticon diode pairs are continuous, spatial structure smaller than 1-pixel element (~10 × 10 sec of arc) is smoothed in the azimuthal direction. In the present nominal operating mode, the barrel scan rate is adjusted so that the image is critically sampled in the azimuthal direction at a resolution of 20 sec of arc.

Each microprocessor is responsible for two of the analog data channels, channels 1–4. Data are transferred from the microprocessor memory into a special portion of the PDP-11/10 core in blocks of 1152 words. These data are then ready for access by the PDP-11/10 command and control program for transmission to magnetic tape.

The primary task of the rest of the K-III data system is the transmission of data from the digital demodulation system to magnetic tape. Each position angle sample of the coronal contributes 128 data points along a radial scan for each sensor. There are four channels, a single-position angle observation is obtained every $^4/_{30}$th of a second, and there are 3 words of 16 bits for each point $pB(r,\theta)$. The effective bit rate is approximately 182 kbits/sec when both microprocessors are working in parallel. These data are written on 1600-bits/in. nine-track magnetic tape in records of 1152 words plus a data header. The header contains 128 words (housekeeping data, position angle, time, data status, etc.). Two records and two interrecord gaps are written for each position angle sampled; the tape consumption rate is 35.25 in./sec. A single 731-m (2400-ft) magnetic tape is filled, regardless of the mode of scan, every 20 min of observation. A data compression technique is available to the site crew which reduces the effective word length from 16 bits to ~4.5 bits per word. This is done at the expense of precision, since reconstruction can only be accomplished to ~10% accuracy and with an increased cost in computer usage at the time the data tapes are used to produce pB images. Data compression is used during periods of low solar activity or during marginal observing conditions.

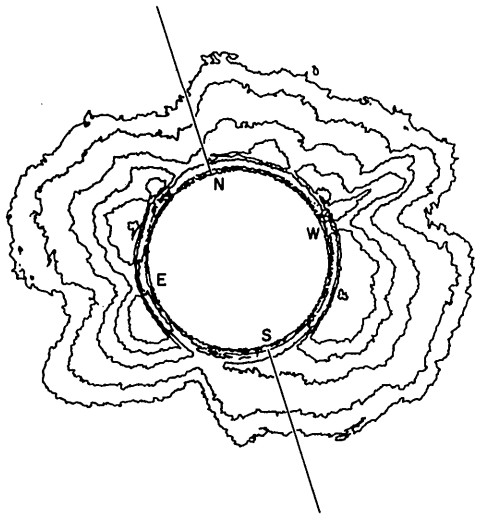

Fig. 3. Real-time contour map of $pB(r,\theta)$ for 5 Aug. 1980, 17:45 UT. Note the large coronal transient on the east limb of the sun.

The K-III barrel may be rotated through an angle of more than 360° so as to achieve a full limb scan. The scan pattern is controlled by the PDP-11/10 and consists of a clockwise rotation followed by a counterclockwise rotation. Observing modes are simply implementations of this idea, with control parameters entered by the observer. The PDP-11/10 system also prepares real-time data displays to give optimal telescope pointing, aid SMM operations, and allow surveillance of the data quality. Real-time data are displayed on graphics terminals. An example is shown in Fig. 3, a contour map of $pB(r,\theta)$.

VII. Prominence Monitor

The Prominence Monitor (P-MON) telescope is a conventional singlet-objective coronograph which may be used to make sequential observations of either the limb or disk near λ6563 A. The elements of the optical system are shown in Fig. 4. The primary image is formed near a rotating six-station wheel which carries three occulting disks, a calibration filter, and two open ports. The telescope is folded up inside the 3-m spar so that the solar image and the image of the objective are brought to focus along the coudé instrument pedestal. The Lyot stop is placed just in front of the

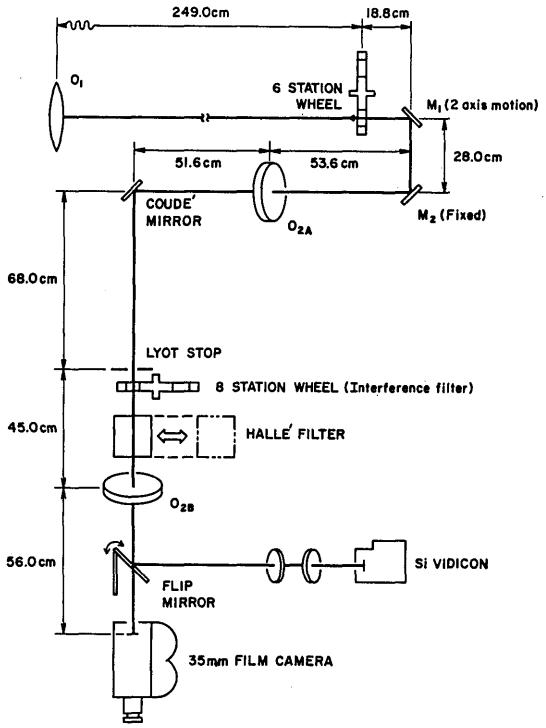

Fig. 4. P-MON optical schematic.

disk to the center of the O_1. Reocculting is accomplished by choosing a disk that is offset by either 1.25 R_0 or 2.00 R_0—these are located on the six-station wheel—and then fine pointing the telescope and rotating the occulting disk about the optical axis until the image is both positioned and occulted correctly in terms of the region of interest.

Both limb and disk observations are required. The bandpass filter centered on H_α is used for limb observations and is also used as a prefilter for a Halle birefringent filter. The birefringent filter may be placed in the beam for disk observations or removed for broadband limb observations. Limb observations may be made with the birefringent filter in either a ½-A FWHM or 1-A FWHM configuration, but exposure times are longer than 500 msec. Four other broad bandpass interference filters are located in the eight-station filter wheel and are displaced ±8 A and ±16 A from the H_α filter. These filters may be used to make line of sight velocity determinations on ejected prominence material using simplifying assumptions about the prominence line profiles. If a limb event is observed with this set of filters and is, in fact, observable in two adjacent filter images, it is possible to infer both total brightness and an effective wavelength for each point in the image $\lambda/\Delta\lambda$ of each filter is ~800, so that if a given

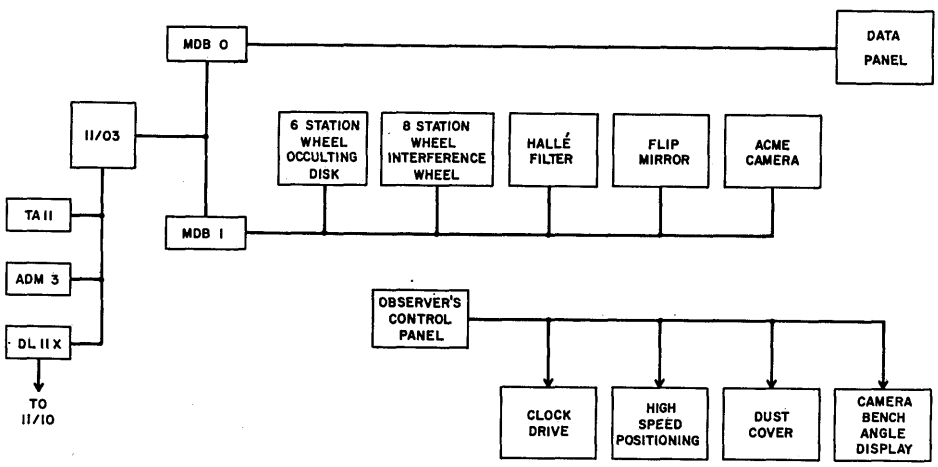

Fig. 5. P-MON electronic systems diagram.

eight-station broad bandpass filter wheel, the final solar image is brought to focus in the film plane of a 35-mm Acme camera. A separate relay system may be used to select the solar image for a real-time video system. Since the coudé bench is fixed in space, both the Acme and video cameras are mounted so that they rotate about the polar axis at the rate of 1 rev/24 h. This is necessary to compensate for apparent image rotation.

The telescope may be pointed independently of the spar and K-III guiding axis, so that large prominance events may be observed at considerable height above the limb. The film format has a total field of view of 3 R_0 by 4 R_0. By offset pointing of the P-MON telescope it is possible to observe to a height of almost 3.5 R_0 for either the east or west limbs. The choice of offset pointing requires the selection of an occulting disk that is offset from the axis connecting the center of the solar image point shows multiple peaks in its distribution of brightness as a function of wavelength, this particular method of inferring line of sight velocities will yield invalid results. On the other hand, this method is sufficiently accurate to infer the gross mass and kinetic energy characteristics of limb events, the existence of helical motions of prominences, etc.

Observing with the P-MON telescope is relatively straightforward and is controlled with a second machine, a PDP-11/03. A systems diagram is shown in Fig. 5. The PDP-11/03 is interfaced to six specific devices: the four-station calibration wheel, six-station occulting wheel, the eight-station filter wheel, the Halle birefringent filter, the flip mirror for Acme/video camera selection, and the Acme camera. The Acme camera control consists of two functions, initiation of an exposure and adjustment of exposure time. By

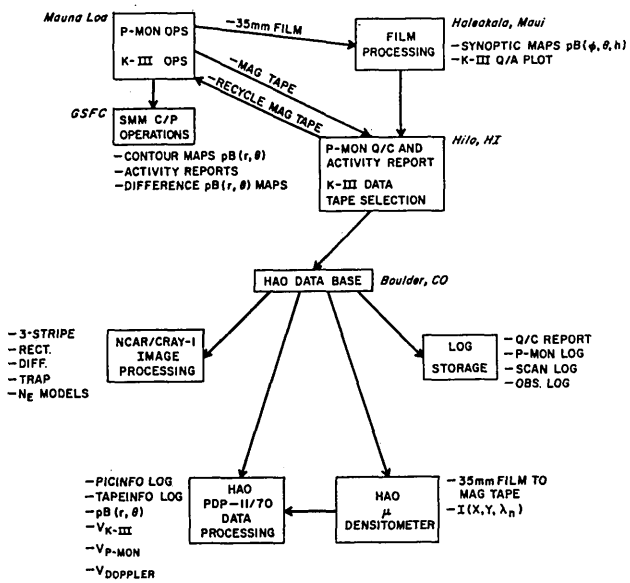

Fig. 6. Coronal dynamics project data system.

identifying the necessary status of each of these components, it is possible to build up a set of instrument conditions and construct a specific observing program.

VIII. Data Management System

The relatively high data rates of both the K-III and P-MON systems require close management of the data kept for scientific analysis. The data path and management system are shown schematically in Fig. 6, along with the locations of various activities.

At the Mauna Loa site it is expected that a 5-h observing day may produce as many as fifteen digital data tapes from K-III and as much as 12 m (40 ft) of undeveloped P-MON 35-mm film. By using the real-time data products from both instruments, the observing logs and the computer compiled instrument log, this initial scientific data set is edited for the selection of the best quality K-III data tape for a single synoptic observation of the K-corona, and to retain those data tapes regarded as being likely to contain observations of coronal activity. A limb event usually is recorded on one compressed data mode tape or about five uncompressed tapes. Magnetic tape culled from a day's observing run is retained at the MLO site for rerecording at a later date. Culled date, the K-III synoptic observation (one tape), the activity data from K-III, and the activity film form P-MON, make up one day's data and are forwarded to Boulder for further reduction and analysis.

At the Boulder site a further reduction of the raw data tapes is accomplished using the HAO and NCAR computing equipment. Information on the K-III data tapes is used to construct a film containing a series of raster scans of Q as a function of height above the limb and position angle. Original data are retained on magnetic tape and, for a shorter period of time, on the Terabit Memory System associated with the Cray-1 computer.

After undergoing this initial step of reduction, tapes are subjected to analysis routines using PDP-11/70 data processing equipment. These provide standard data products such as pB (height) vs azimuth plots, pB histograms as a function of time, and gray scale 35-mm photographic film output of $pB(r,\theta)$. The gray scale plots are written so that a separate archival gray scale plot of each raster is available. Further, this image is of sufficient photometric quality that it may be used to recover the original data by a process of microdensitometry, with some loss of precision incurred. This film archive is retained as the final data product.

Undeveloped P-MON 35-mm film is processed and placed in archival status. The P-MON instrument log provides a catalog of observations by day, pointing parameters, and instrument mode. P-MON films are digitized as they are needed, and these tapes subjected to standard analysis routines for $I(x,y)$ and line of sight velocity $V(x,y,z)$.

The data flow from the MLO instruments into the HAO archive is also shown in Fig. 6. Several different kinds of data product are shown in Figs. 7–9.

IX. Conclusion

The two new coronagraphs have been operational since 4 Feb. 1980. Support for the SMM project has taken the form of telecopy contour plots of the distribution of material in the lower corona, voice messages, and telex alert messages. In several cases, common solar events have been observed in common with other instruments with overlapping fields of view thus achieving the goal of a collaborative observing program. Several significant solar events have been observed in the lower corona by the Mauna Loa systems, and it has been demonstrated that the new equipment will meet the needs of the coronal dynamics project in terms of both sufficient quantity of data of an appropriate quality.

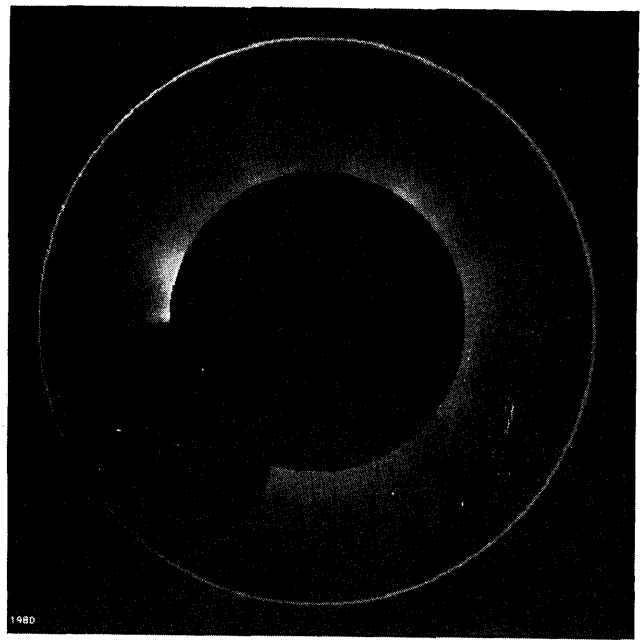

Fig. 7. Rect image of a double eclipse. The digital data are replayed to produce an image that resembles the corona surrounding the sun's dish. The shadow of the moon is seen against the solar corona; the dish of the sun is blocked by the artificial eclipse of the K-III coronagraph. Images of this partial phase of an eclipse provide a rigid test of theoretical spatial resolution (20 sec of arc), scattered light, and final magnification. Geocentric north is toward the top of the frame, geocentric east is to the left.

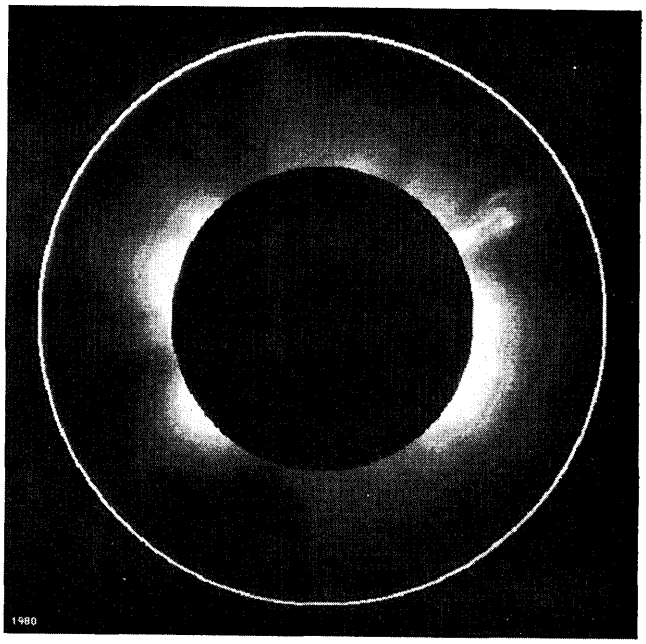

Fig. 9. Diff image showing a large solar transient associated with an eruptive prominence. The Diff image is the result of subtracting two pB images in order to eliminate all coronal features common to both. In this case Diff($r\theta$) = $pB(r,\theta$,19:26 UT) − $pB(r,\theta$,18:05 UT). The dark features represent volumes which have electron densities which are depleted, bright areas originate from volumes of enhanced electron density, gray areas represent portions of the image where no density fluctuations occurred.

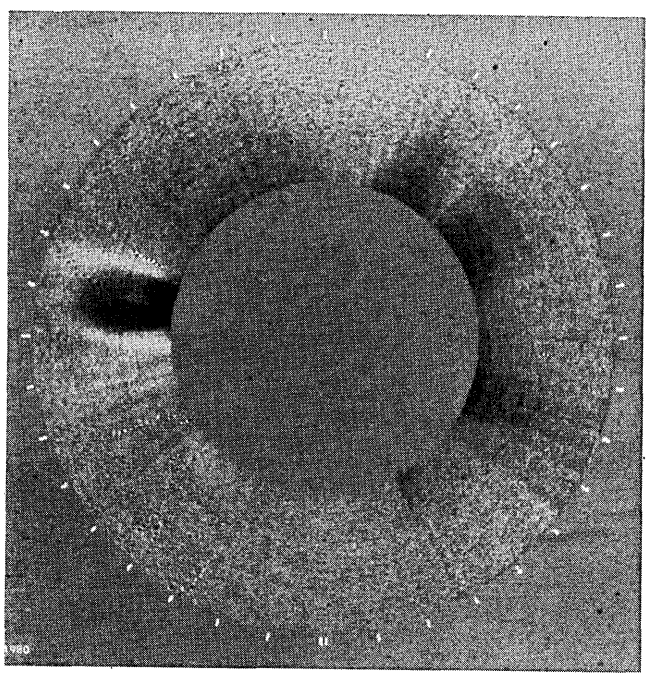

Fig. 8. Rect image of a large transient event in the solar corona. This playback image may be compared directly with the real-time coronal pB contour map shown in Fig. 3.

This new set of instrumentation exists because of the unfailing support provided by J. Firor and the National Center for Atmospheric Research. Major contributions were made by L. Lacey and L. Laramore (mechanical) and H. Hull, E. Harper, S. Rogers, A. Smith, and C. Muir (electronics). The installation phase of this project was performed by the site crew, C. Garcia, E. Yasukawa, F. Telang, K. Rock, and G. Muir. The HAO Forth code was devised by P. Seagraves, Cray-1 software was developed by F. Everts.

The National Center for Atmospheric Research is sponsored by the National Science Foundation.

References

1. G. Wlerick and J. Axtell, Astrophys. J. **126**, 253 (1957).
2. C. Garcia, R. Hansen, H. Hull, and L. Lacey, B.A.A.S. **3**, 261 (1971).
3. R. Kopp, R. Hansen, and R. H. Lee, "A Ground-Based Coronal Dynamics Observing Program for Solar Cycle #21" (1974).
4. J. H. Rush and G. K. Schnable, Appl. Opt. **3**, 1347 (1964).
5. K. Serkowski, in *Planets, Stars and Nebulae*, T. Gehrels, Ed. (U. Arizona Press, Tucson, 1974), p. 135.
6. J. Leroy, R. Muller, and P. Poulain, Astron. Astrophys. **17**, 301 (1972).
7. P. Kuttner, Appl. Opt. **15**, 1199 (1976).
8. W. C. Livingston, J. Harvey, C. Slaughter, and D. Trumbo, Appl. Opt. **15**, 40 (1976).